Nature of the surface states at the single-layer graphene/Cu(111) and graphene/polycrystalline-Cu interfaces

S. Pagliara,[1] S. Tognolini,[1] L. Bignardi,[2,*] G. Galimberti,[1] S. Achilli,[3] M. I. Trioni,[3]
W. F. van Dorp,[2] V. Ocelík,[2] P. Rudolf,[2] and F. Parmigiani[4,†]

[1]*I-LAMP and Dipartimento di Matematica e Fisica, Università Cattolica, 25121 Brescia, Italy*
[2]*Zernike Institute for Advanced Materials, University of Groningen, Nijenborgh 4, 9747AG Groningen, The Netherlands*
[3]*Dipartimento di Chimica, Università degli Studi di Milano and CNR-ISTM, via Golgi 19, 20133 Milano, Italy*
[4]*Università degli Studi di Trieste - Via A. Valerio 2, Trieste 34127, Italy*
Elettra - Sincrotrone Trieste S.C.p.A, Strada Statale 14, km 163.5, 34149 Basovizza, Trieste, Italy
International Faculty - University of Köln, Germany

(Received 9 June 2014; revised manuscript received 16 April 2015; published 27 May 2015)

Single-layer graphene supported on a metal surface has shown remarkable properties relevant for novel electronic and optoelectronic devices. However, the nature of the electronic states derived from unoccupied surface states and quantum well states, lying in the real-space gap between the graphene and the solid surface, has not been explored and exploited yet. Herein, we use ultraviolet nonlinear angle-resolved photoemission spectroscopy to unveil the coexistence at the graphene/Cu(111) interface of a highest occupied Shockley surface state (HOSS) and the two lowest unoccupied surface states (LUSS). The experimental results and electronic structure calculations, based on one-dimensional model potential, indicate that the two unoccupied states originate from the hybridization of an $n = 1$ image potential state with a quantum well state. The hybridized nature of these unoccupied states is benchmarked by a similar experiment done on single-layer graphene grown on copper polycrystalline foil where only the image state survives being the quantum well state at this interface inhibited.

DOI: 10.1103/PhysRevB.91.195440 PACS number(s): 73.22.Pr, 73.20.−r, 78.67.Wj

I. INTRODUCTION

Graphene/metal interfaces have been the subject of extensive studies to understand the substrate-induced perturbation on the graphene electronic structure, in particular in the vicinity of the Dirac cone. The current state of the art distinguishes between strong and weak interactions of graphene with a metal surface [1–8]. A strong interaction, such as with Ru and Ni, alters the occupied states of graphene and the π band shifts to higher binding energy, while the features of the Dirac cone dissolve [1,7,9]. Instead, for graphene deposited on a weakly interacting substrate, e.g., Ir and Cu, the π band is almost unperturbed and the Dirac cone is well defined, while a small doping effect slightly shifts the Fermi level [1,10–12]. These studies provide a comprehensive understanding of the nature and the character of the occupied states of the graphene/metal interface. In contrast, the unoccupied electronic states and, in particular, the nature of the image potential states (IPS) in these systems are still unclear.

IPS are formed by the image potential that results from the charge polarization induced by an electron in front of a metal surface. The wave function of these states is localized at the surface and, in the presence of a gap in the surface-projected bulk bands, it decays exponentially into the solid [13,14]. IPS were observed in literature both in weakly and strongly interacting graphene/metal systems. In the former, the IPS appear also in the presence of graphene [15–17] as for the clean surfaces. On the contrary, in strongly interacting systems that display a single domain orientation and a high corrugation value, two $n = 1$ IPS are observed due to the presence in the sample of two regions with two different graphene/metal distances as for Ru(0001) [9,18,19].

Graphene/Cu(111) is a prototypical example of a weakly interacting system where a single-layer graphene grows forming different domains with a low corrugation and with several azimuthal orientations, nevertheless the average graphene-Cu distance is the same for all domains and comparable to the graphene distance in graphite [1]. Therefore, similarly to graphene/Ir(111) [16], a single series of IPS, unmodified by the presence of graphene, is expected.

Hereafter, we report on a detailed and ultraviolet nonlinear angle-resolved photoemission spectroscopy study of the occupied and unoccupied surface states at the single-layer graphene/Cu(111) interface. We attribute the origin of the two unoccupied surface states to the hybridization of the $n = 1$ IPS with a quantum well state (QWS), lying in the real-gap space between the graphene and the solid surface. This interpretation is strengthened by electronic structure calculations based on a one-dimensional model potential. These calculations suggest that the hybridization between the IPS states and the QWS gives rise to two interface states with an amplitude probability in correspondence of graphene/metal well.

To further prove the QWS character of these states, we have studied the nonlinear angle-resolved photoemission resulting from a graphene single-layer grown on polycrystalline copper (graphene/Cu-poly). At this interface, a single unoccupied imagelike state, not measured on the clean substrate, is detected. In this framework, the results relative to graphene/Cu-poly can be justified considering that the absence of an energy gap in the polycrystalline Cu hinders the QWS generation, but the presence of the graphene potential barrier allows to the image potential to survive giving rise to a single unoccupied imagelike state. By unveiling the nature and the QW character

*Current address: Physikalisches Institut, University of Münster, Wilhelm-Klemm-Str. 10, 48149 Münster, Germany (DE).
†fulvio.parmigiani@elettra.trieste.it

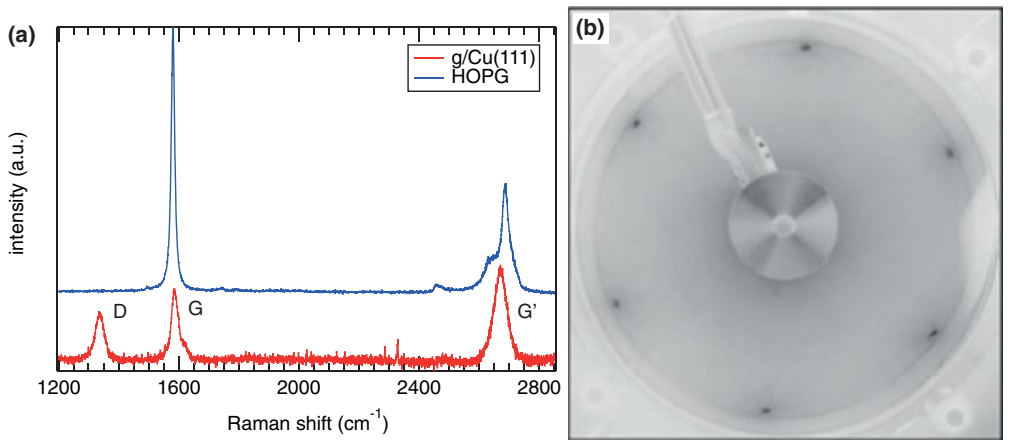

FIG. 1. (Color online) (a) Representative Raman spectrum of graphene/Cu(111) and of HOPG. The relevant peaks of the graphene spectrum are marked. The excitation wavelength employed was $\lambda = 633$ nm. (b) Low-energy electron diffraction pattern of graphene/Cu(111) collected with a primary beam energy of 80 eV.

of the unoccupied surface states at the graphene/Cu(111) single-layer graphene interface, we disclose the potential interest of this system and probably other similar systems as potential optical devices for active and passive optical processes.

II. SAMPLE PREPARATION AND CHARACTERIZATION

Graphene was grown on a Cu(111) single crystal (MaTeck GmbH) that was previously Ar sputtered (1 keV) and annealed (650 K) in ultrahigh vacuum. The crystal was then transferred (through air) into a vacuum furnace (base pressure 10^{-5} mbar), where it was reduced in a mixture of 0.5 mbar of hydrogen (Messer, purity 5.0) and 0.1 mbar of argon (Linde, purity 5.0) for 4 h at a temperature of 1250 K before graphene was grown by exposure to a mixture of argon (0.1 mbar), hydrogen (0.5 mbar), and methane (0.5 mbar, Messer, purity 4.0) for 2 min while the substrate was kept at 1250 K. Graphene was subsequently cooled to room temperature in an argon flow (0.09 mbar) at a rate of 15 K/min. The Cu foil (thickness 25 μm, 99.999 % purity, ESPI Metals) was pre-etched in a 0.25 M solution of H_2SO_4 in water for 5 min, rinsed in water and ethanol, dried in an argon flow and transferred to the vacuum furnace. The foil was then reduced in H_2 and Ar for 1 h at the same temperature and pressure employed for Cu(111), while the growth of graphene followed the same protocol described above for the growth on Cu(111).

For nonlinear angle-resolved photoemission measurements (NL-ARPES), a Ti:Sapphire laser system delivering 0.8 mJ, 150 fs pulses at a wavelength of 790 nm and 1 kHz repetition rate was employed. The laser pulses were also used to pump a traveling wave optical parametric amplifier covering a wavelength range from 0.80 to 1.07 eV. By quadrupling the output of the parametric amplifier, the photon energy could be tuned continuously from 3.20 to 4.28 eV. The near-UV pulses were focused on the sample, kept in an UHV chamber at a residual pressure $\leqslant 2 \times 10^{-10}$ mbar and annealed before the photoemission experiments to 650 K to remove any possible surface contaminants adsorbed during the sample manipulation in air. Photoelectrons were detected by means of a custom-made time of flight (ToF) electron spectrometer with an angular acceptance of $\pm 0.85^\circ$ and an overall energy resolution of $\sim$35 meV at an electron kinetic energy of 2.0 eV. The experimental geometry and the available photon energies allowed the investigation of the parallel crystal momenta in a range of ± 0.3 Å^{-1} around $k_\parallel = 0$ (normal emission). The angle of incidence of the laser beam with respect to the surface normal was $\theta = 30^\circ$. Therefore, while for the s-polarized light beam the electric field E is parallel to the sample surface (horizontal component), the p-polarized beam displayed a horizontal component given by $E_h = |E| \cos\theta$ and a vertical component given by $E_v = |E| \sin\theta$. All measurements were carried out at room temperature.

To characterize the graphene layer, Raman measurements were carried out with a Renishaw inVia μ-Raman, equipped with a 633-nm He-Ne CW laser. The resulting spectrum is shown in Fig. 1(a), together with a spectrum acquired on HOPG for comparison. We identified three main peaks at 1336, 1586, and 2670 cm^{-1}, labeled D, G, and G′, respectively. The G and G′ peaks are characteristic of a graphitic layer [20]. The G′ could be fitted with a single Lorentzian (width $= 49 \pm 7$ cm^{-1}), indicating that a single layer of graphene grew on the copper surface [21]. Collecting maps of 40×40 μm^2, no evidence of domains with two or more or without graphene layers emerges from the μ-Raman spectra of graphene/Cu(111). The presence of a D peak with an intensity comparable to the G peak suggests the presence of grain boundaries and defects in the layer [22]. Moreover, the Raman energy shift of the G mode, benchmarked with free standing graphene, suggests that the graphene layer is n-doped with the Fermi level downward shifted of $\sim$200 meV, in agreement with a single-layer graphene-Cu(111) distance of $\sim$3.2 Å [7,23].

A low-energy electron diffraction pattern [Fig. 1(b)] collected on graphene/Cu(111) shows the hexagonal first-order spots of Cu(111) (surface lattice parameter 2.55 Å) and a ring pattern, for which the corresponding lattice parameter matches that of graphene (2.46 Å). Therefore the graphene crystalline domains do not exhibit any preferential orientation.

The crystalline orientation of the copper foil substrate was checked by electron-back-scattering diffraction. Crystalline domains with sizes ranging from 100 to 1000 μm with a

FIG. 2. (Color online) (a) Electron back scattering diffraction map acquired on a graphene grown on Cu foil sample. (b) Orientation distribution of the image reported in (a). The dominant crystalline orientation is (001).

dominant crystalline orientation close to (001) were observed (see Fig. 2).

III. EXPERIMENTAL RESULTS

The nonlinear photoemission spectrum of the single-layer graphene/Cu(111), acquired with p-polarized light and with photon energy $h\nu = 4.10$ eV, is shown in Fig. 3. The laser photon energy has been tuned up to select $h\nu = 4.10$ eV to unambiguously reveal the emissions originating from the occupied and unoccupied states in the energy region around the Fermi energy (EF), as shown in Fig. 3(b). The d band of Cu(111) was identified at about $E - E_F = 6$ eV with a work function of 4.1 ± 0.1 eV. Moreover, three features were observed and labeled as lowest unoccupied surface states,

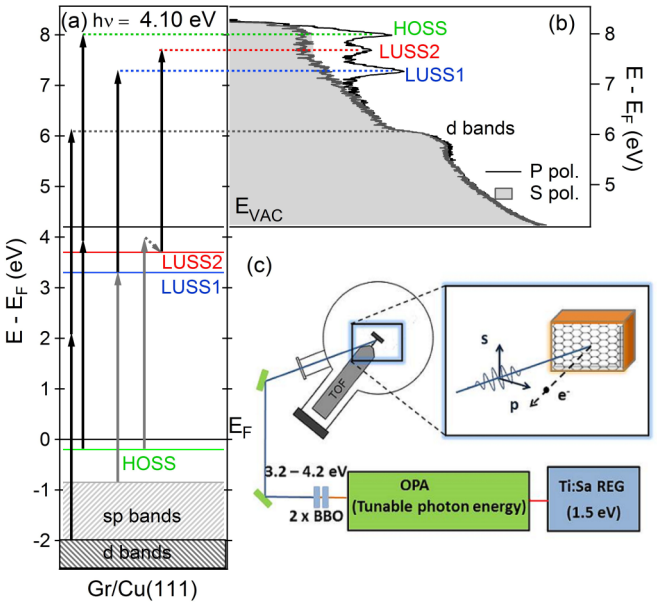

FIG. 3. (Color online) (a) Photoemission processes (arrows) from the Cu d band and from the surface states (HOSS, LUSS1, LUSS2, see text) at the single-layer graphene/Cu(111) interface. (b) Nonlinear photoemission spectrum obtained by using the experimental setup shown in (c), at normal emission ($k_\parallel = 0$) and with a photon energy of 4.10 eV. The HOSS, LUSS1, and LUSS2 emissions, observed with p-polarized light, are completely quenched in the s-polarized light spectrum.

LUSS1 (7.3 eV) and LUSS2 (7.7 eV), and highest occupied surface state, HOSS (8.0 eV). Notably, these emissions are quenched when the laser beam was s polarized [see Fig. 3(c)]. This finding is consistent with the electric dipole selection rules for surface states [24,25].

Figure 4(a) shows the linear emission from the surface occupied states as measured with a photon energy of 6.28 eV. As expected, only the Cu(111) occupied Shockley surface state was observed as a distinct peak at ~0.2 eV just below the Fermi level. This spectral feature is helpful to unambiguously identify the HOSS emission, detected in the nonlinear photoemission spectrum (see Fig. 3), as the Cu(111) Shockley surface state. The shift of the HOSS binding energy with respect to clean Cu(111) is consistent with that measured in conventional angle-resolved photoemission experiments [26–28] and is assigned to a charge-transfer process induced by the different work functions between the graphene layer and the metal surface. This assignment matches also with previous results reported for graphene/Ir(111) [16,17], where an unquenched Shockley state was observed due to the large adsorption distance (~3.4 Å) between metal and graphene.

The energy dispersion $E(k_\parallel)$ for the HOSS state, measured in linear ARPES is reported in Fig. 4(b). The HOSS effective mass derived from the fitting of the $E(k_\parallel)$ data with a parabolic function, was found to be $m^* = 0.45 \pm 0.05\, m_E$, m_E being the free electron mass. This value is consistent with the value of $0.47 \pm 0.04\ m_E$ measured for the Shockley surface state on clean Cu(111) [24,26,27]. Moreover, the intrinsic linewidth at $k_\parallel = 0$ (70 ± 5 meV), obtained by fitting the HOSS with a Lorentzian function convoluted with a Gaussian broadening, accounting for the experimental resolution, was found to be consistent with the value measured on the clean metal (60 ± 10 meV) [24,26].

Considering the linear photoemission spectrum reported in Fig. 4(a), we tentatively assign the LUSS1 and LUSS2 emission in Fig. 4(c) to the unoccupied states of the single-layer graphene/Cu(111). The binding energy (with respect to the vacuum level) of LUSS1 and LUSS2 was 0.90 ± 0.05 and 0.50 ± 0.05 eV, respectively, while the intrinsic linewidth at $k_\parallel = 0$ was found to be 115 ± 5 meV for LUSS1 and 140 ± 5 meV for LUSS2. The multiphotonic order (MPO) measured from the nonlinear photoemission spectra collected at $h\nu = 4.10$ eV and $k_\parallel = 0$, is MPO=2. This is the value expected for a second-order nonlinear photoemission process where the first photon transiently populates the LUSS1 and LUSS2 states from the Cu(111) occupied states, while a second photon is providing the energy for the electron emission. The effective masses of LUSS1 and LUSS2, evaluated from nonlinear ARPES at $h\nu = 4.10$ eV, were found to be $m^*_{\mathrm{LUSS1}} = 0.9 \pm 0.1\ m_E$ and $m^*_{\mathrm{LUSS2}} = 1.3 \pm 0.1\ m_E$ [see Fig. 4(d)]. Instead, the HOSS effective mass measured at $h\nu = 4.10$ eV matches the value obtained by linear ARPES reported in Fig. 4(b).

Figure 5 shows nonlinear photoemission spectra ($h\nu = 4.10$ eV) measured on the single-layer graphene on the Cu foil and on clean Cu foil. On the clean Cu foil we detected only the emission originating from the Cu d band along with a clear Fermi edge. The presence of a continuum of states at the Fermi level without any energy gap in the integrated projected band structure of the Cu foil hinders, as expected,

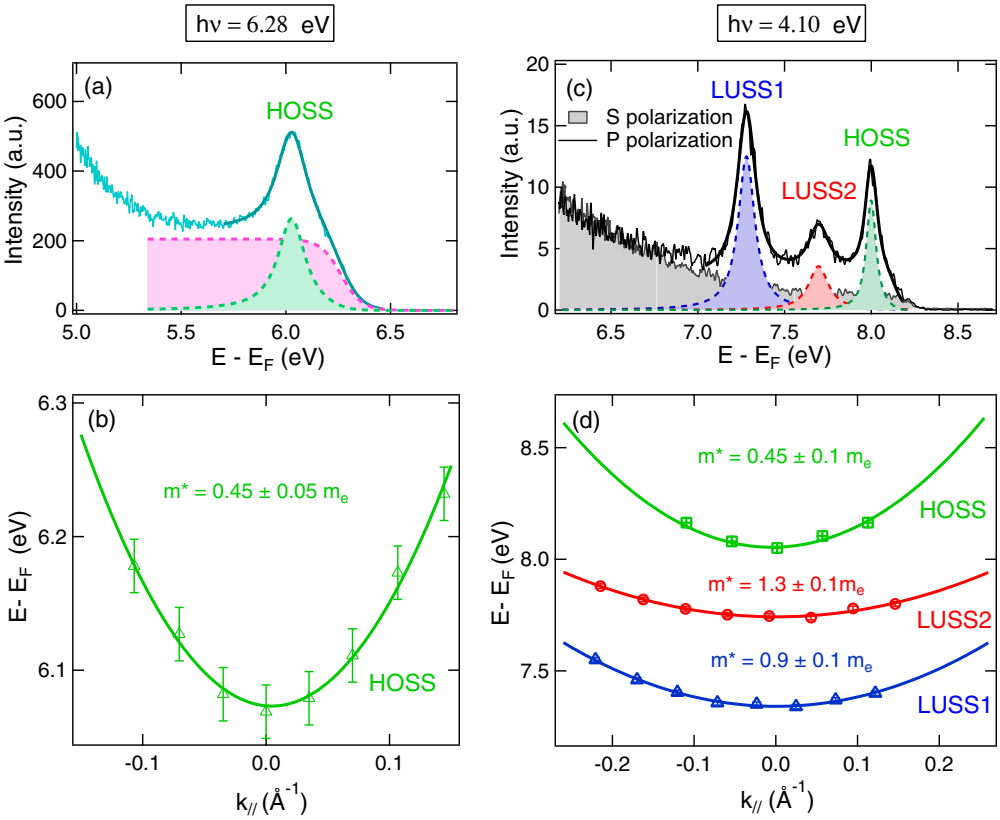

FIG. 4. (Color online) (a) Linear photoemission spectrum collected at normal emission ($k_\parallel = 0$) with a photon energy of 6.28 eV and p-polarized light at the single-layer graphene/Cu(111) interface. (b) Energy position vs $k_\parallel$ momentum for the Shockley surface state measured at $h\nu = 6.28$ eV. A parabolic fit (line) gives an effective mass of $0.45 \pm 0.05\, m_E$. (c) Single-layer graphene/Cu(111) nonlinear photoemission spectra measured at normal emission ($k_\parallel = 0$) in p and s polarization and 4.1 eV photon energy. The p-polarized spectrum results well interpolated by three structures. (d) Energy position vs $k_\parallel$ momentum for the Shockley surface state (HOSS), LUSS1, and LUSS2 interface states measured at $h\nu = 4.10$ eV photon energy. The effective masses reported in the figure are obtained from the parabolic fit (line) of the measured band dispersion.

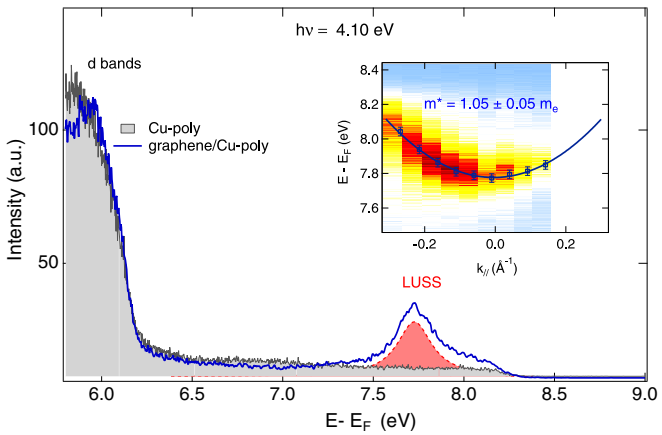

FIG. 5. (Color online) Comparison between nonlinear photoemission spectra measured at $k_\parallel = 0$ using p-polarized laser pulses at $h\nu = 4.10$ eV on graphene grown on polycrystalline Cu foil and on clean Cu foil. The emission measured from the single-layer graphene on the Cu foil detected in the 7.0–8.5 eV E-E_F energy region is well fitted by a single Lorentzian and a Fermi-Dirac function. The inset shows the single-layer graphene/Cu-poly foil LUSS band dispersion. The effective mass for this state is deduced from the parabolic fit (solid line) of the ARPES data.

the formation of image states. Conversely, on single-layer graphene/Cu-poly, beside the d band and the Fermi edge, an additional feature is clearly detected. This state exhibits a surface-state symmetry, vanishing with s-polarized light and an effective mass consistent with the free-electron mass as it is shown in the inset of Fig. 5.

IV. THEORY AND DISCUSSION

Concerning the results obtained on graphene/Cu(111), LUSS1 can be identified with the $n = 1$ IPS of Cu(111), being its binding energy and effective mass comparable to those of a typical first image state in front of a metal surface. Differently, the behavior of LUSS2 is unknown in literature. In principle, we can speculate that LUSS2 was the $n = 1$ state of a second series of IPS. Two series of IPS have been recently observed in the strongly interacting graphene/Ru interface [9]. In this system, however, the morphology of the graphene layer is completely different. The strong corrugation (about 1.5 Å) of the graphene layer produces two different regions (H and L region) responsible for the presence in the spectrum of two $n = 1$ IPS that differ in binding energy of about 150 meV. As often emphasized in literature, graphene/Cu(111) is a prototypical example of weakly interacting system

where graphene grows forming different domains with several azimuthal orientations as confirmed by both Raman and low-energy electron diffraction measurements collected on our sample (Fig. 1). The average graphene-Cu distance is about 3.2 Å for all domains and the maximum corrugation of a single domain is 0.35 Å [29]. The presence of two $n = 1$ IPS that differ in binding energy by about 400 meV could be justified in graphene/Cu only by an important variation of the graphene-Cu distance and consequently of the local work function. From *ab initio* calculations within the density functional theory (DFT) as implemented in the SIESTA package, we estimate that a variation of the local work function of 400 meV can be only justified by a distance variation of 1 Å, suggesting that domains with a graphene-Cu distance of about 2 Å should exist and they must be quite extended.

Two series of IPS could be originated also by a change of the charge transfer sign, from *n* to *p* [30] between the substrate and graphene. However, a significant change in charge transfer must necessarily affect the binding energy of the occupied surface state (HOSS) that in our experiment appears evermore shifted by ∼200 meV with respect to the Fermi level. This observation is based on micro-ARPES experiments performed with a lateral resolution of ∼1 μm [31]. These measurements have shown that the binding energy of HOSS does not change significantly on the whole graphene/Cu(111) surface invalidating this interpretation of the present data.

Hence, having excluded that LUSS2 was a second IPS, to clarify the nature of the LUSS1 and LUSS2 states, we performed electronic structure calculations using the one-dimensional model potential reported in Fig. 6(a). The Cu(111) surface is described by a phenomenological modulated potential, as proposed by Chulkov *et al.*[32,33], which is able to reproduce main surface features of the metal surface such as the experimental work function, the surface-projected energy gap, and the energy position of surface and image states.

To model the potential due to the graphene layer, we used a potential barrier in correspondence with the graphene plane, at 3.2 Å from the Cu(111) surface, plus two potential wells on both sides of the graphene. A similar potential has been already adopted in the literature to simulate graphene [18] because it accounts for the transmission and reflection of electronic wave functions impinging on the carbon layer. In addition, our potential considers the effective barrier on the bulk side, generated by the presence of the energy L gap.

The shape of this additional potential can be chosen in different ways and for sake of computational simplicity we considered a cosinelike attractive well and a cosinelike barrier. Its analytic form in atomic units is

$$v_{Gr}(z) = \begin{cases} A_1\{\cos[2\pi(z+\lambda_T)/\lambda_1]-1\} & -\lambda_T < z < -\lambda_2/2 \\ A_2\{\cos[2\pi z/\lambda_2]+1\}-2A_1 & -\lambda_2/2 < z < 0.75 \end{cases}, \quad (1)$$

where λ_1 and λ_2 are fixed to 2.25 and 2 Bohr, respectively, and $2\lambda_T$ is their sum. A_1 and A_2 are equal to 0.43 and 1.7 Hartree, respectively.

The parameters for the graphene barrier were chosen in order to reproduce the energy levels measured by linear and nonlinear photoemission. This procedure does not uniquely fix the parameters, but we found that different combinations that gave the same energy values resulted in almost equivalent surface wave functions.

The electronic structure calculations were performed using the embedding approach that allows to describe a semi-infinite substrate [34,35]. The density of states reported in Fig. 6(b) displays the continuous bulk states of Cu projected along the [111] direction and an energy gap; in this gap we find three states, with binding energies equal to −4.55, −0.9, and

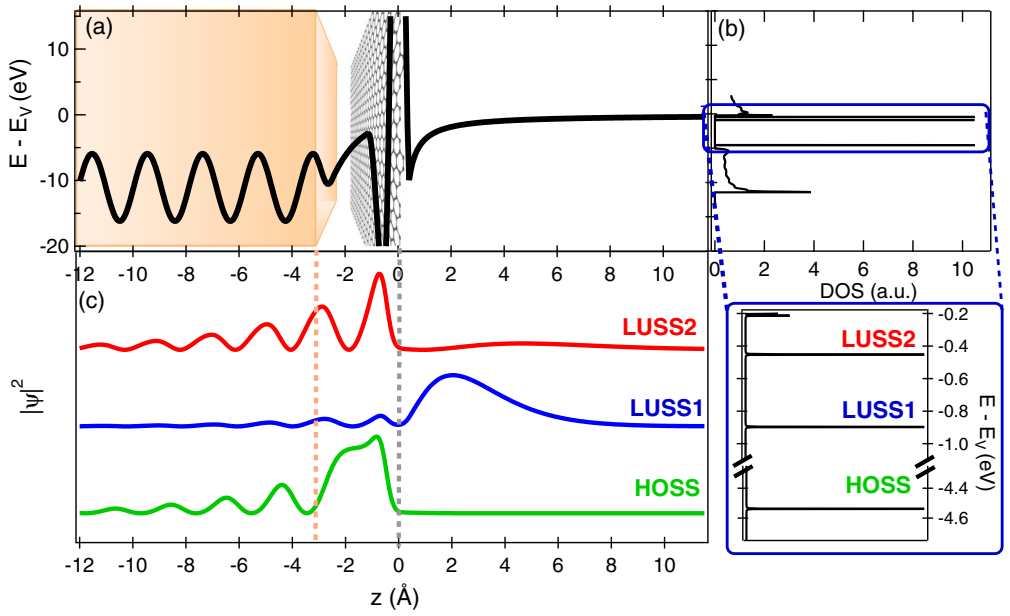

FIG. 6. (Color online) (a) One-dimensional potential used to simulate the graphene/Cu(111) interface. (b) The calculated density of states (DOS) points out the presence of three states whose binding energies are comparable with the HOSS, LUSS1, and LUSS2 binding energies measured in the two-photon photoemission spectrum of Fig. 3. In (c), the probability amplitude of HOSS, LUSS1, and LUSS2 states is plotted.

−0.45 eV with respect to the vacuum level, which can be identified as HOSS, LUSS1, and LUSS2, respectively [see Fig. 6(b)]. The probability amplitude of these states is reported in Fig. 6(c). The HOSS is mainly localized in front of the Cu(111) surface, as expected for a Shockley state. Differently, LUSS1 and LUSS2 present the character of interface states being spatially localized at the graphene/vacuum and the graphene/Cu(111) interfaces. Their proximity in energy suggests that they can be ascribed to the hybridization of two nearly degenerate levels lying in the two potential wells formed by the graphene potential barrier with the surface energy gap and the image potential, respectively. Although LUSS1 and LUSS2 display the same physical nature, the experiments revealed distinct effective masses. The difference between the value of $m^*_{\mathrm{LUSS1}} = 0.9 \pm 0.1\, m_E$ and $m^*_{\mathrm{LUSS2}} = 1.3 \pm 0.1\, m_E$ can be explained by the different energy positions of these states with respect to the bulk band edge. When the binding energy of an unoccupied state is close to the upper edge of the energy gap, the effective mass is affected by the deviation of the band dispersion from the free electron behavior. As explained by the multiple reflection theory approach [36], when moving along $k_\parallel$, this results in a different phase shift of the wave functions reflected by the barrier, represented by the energy gap. Consequently, the effective height of the quantum well in which electrons are trapped changes with $k_\parallel$. In graphene/Cu(111), LUSS1 is sufficiently distant in energy from the band edge to account for a nearly free electron dispersion. Differently, LUSS2 is found at ∼0.2 eV below the band edge, and this energy proximity explains the value of the effective mass $\sim 1.3\, m_E$ within the energy gap. This value is similar to what is observed for the first IPS of the clean Cu(111), which is found close to the bulk band edge because of the higher work function of the clean surface with respect to single-layer graphene/Cu(111) [24,26].

This scenario is confirmed by the single imagelike state (LUSS) detected on graphene/Cu-poly where a single imagelike state (LUSS) not present in the Cu foil appears (see Fig. 5). As previously remarked, the presence of a continuum of states at the Fermi level of the Cu foil without any energy gap in the integrated projected band structure hinders the formation of an image state in the spectrum collected on the Cu foil and similarly prevents the generation of the QWS in the real space between the foil and graphene. At the same time, graphene grown on a foil originates a potential barrier that, conversely to the case of polished Cu foil, blocks the photoemitted electrons back into the metal allowing the formation of the only image state.

V. CONCLUSIONS

The study set forth herein presents a combined experimental and theoretical investigation of the occupied and unoccupied electronic surface states of a single graphene layer on Cu(111) and on Cu-poly surfaces, unveiling at the graphene/Cu(111) interface the coexistence of a highest occupied Shockley surface state (HOSS) and two lowest unoccupied surface states (LUSS). The experimental results, obtained by ultraviolet nonlinear angle-resolved photoemission spectroscopy and the electronic structure calculations, based on a one-dimensional model potential, clearly suggest that the two unoccupied states originate from the hybridization of the $n = 1$ single-layer graphene/Cu(111) image potential state with a quantum well state. This interpretation is confirmed by a similar experiment done on single-layer graphene grown on copper polycrystalline foil where only the image state survives being the quantum well state at this interface inhibited. By adding important information to the present knowledge on the character of the surface states of these interfaces, we also unlock the gate for considering Cu/graphene interfaces and probably other similar systems as basic three-level devices suitable for active and passive optical processes.

ACKNOWLEDGMENTS

This work was supported by the "Graphene-based electronics" research program of the Stichting voor Fundementeel Onderzoek der Materie (FOM), part of the Nederlandse Organisatie voor Wetenschappelijk Onderzoek (NWO). S.P. thanks the MIUR for supporting this work under Contract No. PRIN 2010BNZ3F2 and acknowledges partial support from D.2.2 grants of the Università Cattolica.

[1] M. Batzill, Surf. Sci. Rep. **67**, 83 (2012).
[2] Z. Xu and M. J. Buehler, J. Phys.: Condens. Matter **22**, 485301 (2010).
[3] J. Wintterlin and M. L. Bocquet, Surf. Sci. **603**, 1841 (2009).
[4] C. Gong, G. Lee, B. Shan, E. M. Vogel, R. M. Wallace, and K. Cho, J. Appl. Phys. **108**, 123711 (2010).
[5] L. Colombo, R. M. Wallace, and R. S. Ruoff, Proc. IEEE **101**, 1536 (2013).
[6] F. Carbone, P. Baum, P. Rudolf, and A. H. Zewail, Phys. Rev. Lett. **100**, 035501 (2008).
[7] G. Giovannetti, P. A. Khomyakov, G. Brocks, V. M. Karpan, J. van den Brink, and P. J. Kelly, Phys. Rev. Lett. **101**, 026803 (2008).
[8] P. A. Khomyakov, G. Giovannetti, P. C. Rusu, G. Brocks, J. van den Brink, and P. J. Kelly, Phys. Rev. B **79**, 195425 (2009).
[9] N. Armbrust, J. Güdde, P. Jakob, and U. Höfer, Phys. Rev. Lett. **108**, 056801 (2012).
[10] I. Pletikosić, M. Kralj, P. Pervan, R. Brako, J. Coraux, A. T. N'Diaye, C. Busse, and T. Michely, Phys. Rev. Lett. **102**, 056808 (2009).
[11] M. Kralj, I. Pletikosić, M. Petrović, P. Pervan, M. Milun, A. T. N'Diaye, C. Busse, T. Michely, J. Fujii, and I. Vobornik, Phys. Rev. B **84**, 075427 (2011).
[12] C. Jeon, H.-N. Hwang, W.-G. Lee, Y. G. Jung, K. S. Kim, C.-Y. Park, and C.-C. Hwang, Nanoscale **5**, 8210 (2013).
[13] U. Höfer, I. L. Shumay, Ch. Reuß, U. Thomann, W. Wallauer, and Th. Fauster, Science **277**, 1480 (1997).
[14] S. Hüfner, *Photoelectron Spectroscopy* 3rd ed. (Springer-Verlag, 2003).
[15] P. L. de Andres, P. M. Echenique, D. Niesner, Th. Fauster, and A. Rivacoba, New J. Phys. **16**, 023012 (2014)

[16] D. Niesner, Th. Fauster, J. I. Dadap, N. Zaki, K. R. Knox, P.-C. Yeh, R. Bhandari, R. M. Osgood, M. Petrović, and M. Kralj, Phys. Rev. B **85**, 081402 (2012).

[17] D. Nobis, M. Potenz, D. Niesner, and Th. Fauster, Phys. Rev. B **88**, 195435 (2013)

[18] H. G. Zhang, H. Hu, Y. Pan, J. H. Mao, M. Gao, H. M. Guo, S. X. Du, T. Greber, and H.-J. Gao, J. Phys.: Condens. Matter **22**, 302001 (2010).

[19] B. Borca, S. Barja, M. Garnica, D. Sánchez-Portal, V. M. Silkin, E. V. Chulkov, C. F. Hermanns, J. J. Hinarejos, A. L. Vázquez de Parga, A. Arnau, P. M. Echenique, and R. Miranda, Phys. Rev. Lett. **105**, 036804 (2010).

[20] Y. Gogotsi, J. A. Libera, N. Kalashnikov, and M. Yoshimura, Science **290**, 317 (2000).

[21] A. Ferrari, Solid State Commun. **143**, 47 (2007).

[22] J. D. Wood, S. W. Schmucker, A. S. Lyons, E. Pop, and J. W. Lyding, Nano Lett. **11**, 4547 (2011).

[23] A. Das, S. Pisana, B. Chakraborty, S. Piscanec, S. K. Saha, U. V. Waghmare, K. S. Novoselov, H. R. Krishnamurthy, A. K. Geim, A. C. Ferrari, and A. K. Sood, Nat. Nanotechnol. **3**, 210 (2008).

[24] S. Pagliara, M. Montagnese, S. Dal Conte, G. Galimberti, G. Ferrini, and F. Parmigiani, Phys. Rev. B **87**, 045427 (2013).

[25] M. Wolf, A. Hotzel, E. Knoesel, and D. Velic, Phys. Rev. B **59**, 5926 (1999).

[26] S. Caravati, G. Butti, G. P. Brivio, M. I. Trioni, S. Pagliara, G. Ferrini, G. Galimberti, E. Pedersoli, C. Giannetti, and F. Parmigiani, Surf. Sci. **600**, 3901 (2006).

[27] S. Pagliara, G. Ferrini, G. Galimberti, E. Pedersoli, C. Giannetti, and F. Parmigiani, Surf. Sci. **600**, 4290 (2006).

[28] S. Pagliara, G. Ferrini, G. Galimberti, E. Pedersoli, C. Giannetti, C. A. Rozzi, and F. Parmigiani, Surf. Sci. **602**, 2983 (2008).

[29] P. Süle, M. Szendró, C. Hwang, and L. Tapasztó, Carbon **77**, 1082 (2014).

[30] E. Starodub, A. Bostwick, L. Moreschini, S. Nie, F. El Gabaly, K. F. McCarty, and E. Rotenberg, Phys. Rev. B **83**, 125428 (2011).

[31] S. Gottardi, K. Müller, L. Bignardi, J. C. Moreno-López, T. A. Pham, O. Ivashenko, M. Yablonskikh, A. Barinov, J. Björk, P. Rudolf, and M. Stöhr, Nano Lett. **15**, 917 (2015).

[32] E. V. Chulkov, V. M. Silkin, and P. M. Echenique, Surf. Sci. **437**, 330 (1999).

[33] The two parameters A_{10} and A_2 of the potential that control the work function and the binding energy of the Shockley state have been fixed to $A_{10} = -11.055$ and $A_2 = -2.3279$ in order to account for the changes induced by the graphene sheet in front of the Cu(111) surface.

[34] S. Achilli, M. I. Trioni, E. V. Chulkov, P. M. Echenique, V. Sametoglu, N. Pontius, A. Winkelmann, A. Kubo, J. Zhao, and H. Petek, Phys. Rev. B **80**, 245419 (2009).

[35] S. Achilli, M. I. Trioni, and G. P. Brivio, Phys. Rev. B **81**, 165444 (2010).

[36] N. V. Smith, Phys. Rev. B **32**, 3549 (1985).